Geological Quarterly, 2012, **56** (1): 55–66

Ambiguous geological position of Carboniferous rhyodacites in the Intra-Sudetic Basin (SW Poland) clarified by SHRIMP zircon ages

Ryszard KRYZA and Marek AWDANKIEWICZ

Kryza R. and Awdankiewicz M. (2012) – Ambiguous geological position of Carboniferous rhyodacites in the Intra-Sudetic Basin (SW Poland) clarified by SHRIMP zircon ages. Geol. Quart., **56** (1): 55–66.

Rhyodacite sheets (the Sady Górne Rhyodacites) in the lowermost part of the Permo-Carboniferous Intra-Sudetic Basin molasse fill have been mapped as intrusives but, later on, based on ambiguous field and petrographic evidence, reinterpreted as lower Carboniferous lavas and tuffs; if so, they would mark the earliest episode of late-orogenic volcanism in the Intra-Sudetic Basin and in the whole Sudetes region in SW Poland. However, re-examination of field relationships and new observations are consistent with an intrusive emplacement of the rhyodacites as conformable to semiconformable, simple to composite sheets. SHRIMP zircon study indicates that the rhyodacites contain rare inherited zircons of *ca*. 560 Ma, and *ca*. 470 Ma (or slightly older), and a main population of zircons with an average concordia age of 306.1 ±2.8 Ma. This latter age documents the emplacement of the rhyodacites during a mid/late late Carboniferous (Westphalian) stage of volcanism in the Intra-Sudetic Basin in the Central European Variscides. This post-orogenic volcanism was possibly initiated several million years later than previously assumed, and could have comprised a few pulses over a relatively prolonged time span of millions of years.

Ryszard Kryza, Marek Awdankiewicz, Institute of Geological Sciences, University of Wrocław, Cybulskiego 30, 50-205 Wrocław, Poland, e-mails: ryszard.kryza@ing.uni.wroc.pl, marek.awdankiewicz@ing.uni.wroc.pl (received: April 26, 2011; accepted: November 29, 2011).

Key words: Sudetes, Variscan orogeny, Carboniferous, SHRIMP zircon dating, volcanism, subvolcanic intrusions.

INTRODUCTION

The Intra-Sudetic Basin is the largest and oldest late Paleozoic intramontane basin in the eastern part of the European Variscides (Fig. 1). The basin was initiated as early as in the Visean (Turnau *et al*., 2002) due to Variscan orogenic movements and, up to the late Permian, accommodated several thousand metres of dominantly siliciclastic alluvial deposits (Wojewoda and Mastalerz, 1989; Dziedzic and Teisseyre, 1990; Mastalerz and Prouza, 1995). Intercalations of silicic to intermediate volcanogenic rocks in these molasse deposits document several intra-basinal volcanic events, such as effusions of lava flows and domes from shield-type and compound volcanoes, emplacement of laccoliths and other shallow-level intrusions, as well as ignimbrite eruptions during the climax of volcanism in Permian times (Awdankiewicz, 1999*a*, *b*, 2004 and references therein). However, detailed reconstructions of the volcanic evolution as well as broader-scale regional correlations are hampered by imprecise constraints on the age and timing of the volcanic activity, especially due to the scarcity of isotopic ages obtained from the volcanic rocks. Among the important questions is the timing of the onset of volcanic activity in this part of the Variscan orogen.

The Sady Górne rhyodacites (SGRd; Awdankiewicz, 1999*a*) occur in the lowermost part of the Permo-Carboniferous Intra-Sudetic Basin fill, near the northern margin of the basin. These rocks were initially considered as late Paleozoic intrusive veins (Berg *et al*., 1906; Dathe and Zimmermann, 1912; Zimmermann, 1920), but later were reinterpreted as lower Carboniferous lavas and tuffs (Teisseyre, 1966; Teisseyre, 1972) marking the earliest episode of late-orogenic volcanism in the Intra-Sudetic Basin and in the whole Sudetes region (Teisseyre, 1966; Awdankiewicz, 1999*a*, *b*). Such a geological position made the SGRd an attractive target for SHRIMP zircon geochronology. The dating has been carried out and, surprisingly, the results obtained point to a late, not early Carboniferous age of the rhyodacites. These results falsify the established views on the geological position of the

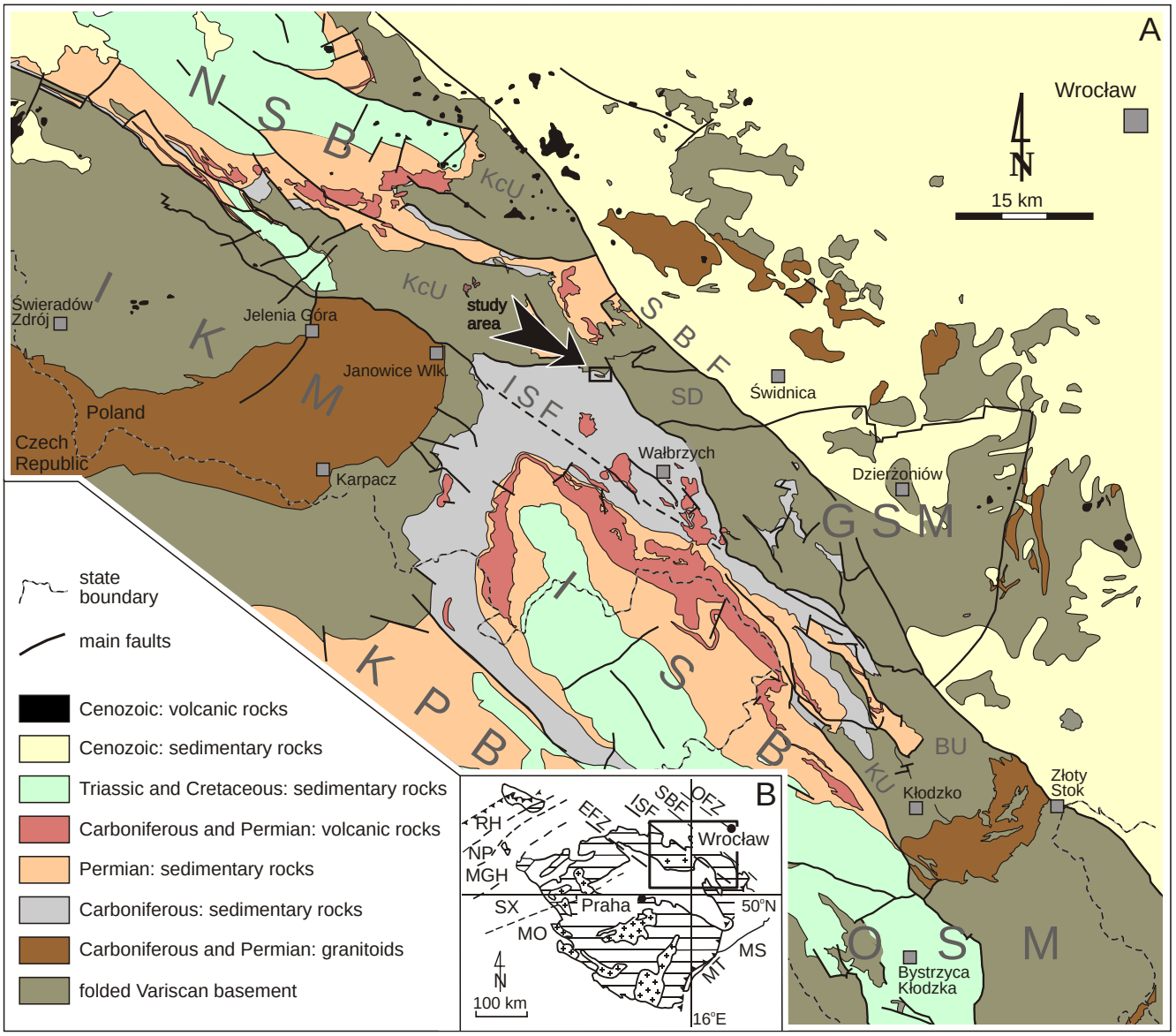

Fig. 1A – geological sketch map of Lower Silesia (modified from Kodym *et al.*, 1967; Bossowski *et al.*, 1981; Sawicki, 1988; Milewicz *et al.*, 1989) showing the distribution of late Paleozoic intramontane basins of the Sudetes: the North-Sudetic Basin (NSB), the Intra-Sudetic Basin (ISB) and the Krkonoše Piedmont Basin (KPB); B – location of the area within the European Variscides

A: BU – Bardo Unit, GSM – Góry Sowie Massif, KcU – Kaczawa Unit, IKM – Izera–Karkonosze Massif, ISF – Intra-Sudetic Fault, KU – Kłodzko Unit, OSM – Orlica–Śnieżnik Massif, SBF – Sudetic Boundary Fault, SD – Świebodzice Depression; **B**: EFZ – Elbe Fault Zone, ISF – Intra-Sudetic Fault, MGH – Mid-German High, MO – Moldanubian Zone, MS – Moravo-Silesian Zone, MT – Moldanubian Thrust, NP – Northern Phyllite Zone, OFZ – Odra Fault Zone, RH – Rheno-Hercynian Zone, SBF – Sudetic Boundary Fault, SX – Saxo-Thuringian Zone, large Variscan granitoid plutons indicated with crosses

rocks dated and, consequently, on the commencement of late Paleozoic volcanism in the Sudetes.

In this paper we: (a) reconcile the published data on the geology of the rhyodacites with new field observations on emplacement-related structures in selected, well-exposed sections, and (b) present the results of SHRIMP zircon dating. These results provide the basis for the discussion of:

- the intrusive *versus* extrusive emplacement mode of the rhyodacites,
- the age of the SGRd and of crustal components involved in the rhyodacite magma formation,
- implications for the timing of late Paleozoic volcanism in this part of Variscan Europe.

METHODS

Re-examination of published data and our own new observations on the field relationships, structures and textures of the Sady Górne rhyodacites are used to critically assess the evidence for an effusive *versus* a subvolcanic origin of the rhyodacite bodies. A zircon morphological study was performed on one sample of the rhyodacites by M. Jurasik within her MSc project (Jurasik, 2006). We used the zircon separate of Jurasik for a SHRIMP geochronological study the results of which are reported in this paper.

The rhyodacite sample, *ca*. 3 kg in weight, was crushed, sieved and heavy minerals separated by a conventional heavy liquid (sodium polytungstate, d = 3.0 g/cm^3) method. Hand-picked zircons representing various morphological and structural types were studied by optical microscope and, afterwards, mounted in resin, ground and polished for CL imaging and *in situ* U-Pb dating. The analyses were performed on the SHRIMP II at VSEGEI, St. Petersburg. The analytical conditions and data treatment procedures were as described in Larionov *et al*. (2004) and are outlined in the Appendix.

GEOLOGICAL SETTING AND PREVIOUS WORK

The Intra-Sudetic Basin is a late Paleozoic intramontane trough situated at the NE margin of the Bohemian Massif (Fig. 1). The basin is filled with a lower Carboniferous–upper Permian molasse succession, overlain by lower Triassic and upper Cretaceous deposits (Nemec *et al*., 1982; Dziedzic and Teisseyre, 1990; Mastalerz and Prouza, 1995). The upper Paleozoic succession comprises up to 6.5 km of lower Carboniferous, 2 km of upper Carboniferous and 1.5 km of Permian deposits. The distribution of these deposits is asymmetric, and the basin fill shows a general thinning and becomes younger south-eastwards. Most of the Permo-Carboniferous deposits are of continental, alluvial origin; lacustrine intercalations are typical of the Permian, and deltaic and marine intercalations of the upper Visean deposits. Acidic to intermediate/basic volcanic rocks form relatively sparse bodies in the Carboniferous deposits and extensive outcrops in the lower Permian deposits. Two stages of volcanism in the early and late Carboniferous, and a climax of volcanic activity in early Permian times have been inferred (Awdankiewicz, 1999*a*, *b*; Ulrych *et al*., 2004 and references therein). Preliminary SHRIMP zircon dating confirmed a late Carboniferous subvolcanic event at *ca*. 310 Ma (Awdankiewicz and Kryza, 2010). The specimen dated was a rhyodacite sampled from the Chełmiec laccolith west of the town of Wałbrzych. Other rhyodacite shallow-level intrusive and extrusive bodies crop out around the Chełmiec laccolith and locally, are also found in the lowermost part of the Intra-Sudetic Basin fill.

The oldest deposits of the Intra-Sudetic Basin, at the base of the succession at the northern margin of the basin, comprise several formations of limited lateral extent, including the Sady Górne Formation. This formation is up to 600 m thick and comprises conglomerates with intercalations of mudstones and sandstones. Correlation with laterally equivalent formations dated by miospore findings points to the accumulation of the Sady Górne Formation in the Holkerian Stage of the Visean (Turnau *et al*., 2002) which, in the current stratigraphic subdivisions for Poland and Europe (Wagner, 2008), corresponds to the early late Visean (*ca*. 334–333 Ma). This dating constrains also the onset of late orogenic sedimentation in the Intra-Sudetic Basin (Turnau *et al*., 2002). These oldest deposits accumulated in a narrow, E–W trending graben bordered by active faults, with alluvial fans along the margins feeding an axial fluvial system (Teisseyre, 1968, 1975; Dziedzic and Teisseyre, 1990). The clastic material of the Sady Górne Formation comprises local detritus derived from the adjacent Kaczawa Unit to the north and the Świebodzice Depression and the Góry Sowie Massif to the east and south-east, with significant "tuffaceous" admixture (Teisseyre, 1970; see also below).

This paper deals with the Sady Górne rhyodacites (Awdankiewicz, 1999*a*), which crop out in the upper part of the Sady Górne Formation. The rhyodacites and their country rocks were mapped in detail by Berg *et al*. (1906), Teisseyre (1966) and Teisseyre (1972). Teisseyre (1966) used trenches extensively in this poorly exposed area, and his results were partly incorporated in Teisseyre's (1972) map. Relevant sections of the two 1:25 000 maps (Fig. 2A, B) differ in some important aspects. This is partly due to the generalization of two main rhyodacite outcrops into a single outcrop in the more recent, 1972 map. Other differences, however, include:

- the absence or presence of tuffs near the base of the main rhyodacite outcrop;
- the unconformable or conformable position of the western part of the main rhyodacite outcrop relative to sedimentary formation boundaries.

Berg *et al*. (1906), Dathe and Zimmermann (1912) and Zimmermann (1920) considered that the "porphyries" they mapped are intrusive veins, up to 20 m thick, of late Carboniferous or Permian age. However, Teisseyre (1966) reinterpreted the "porphyries" as lavas and tuffs of early Carboniferous age, contemporaneous with the adjacent lower Carboniferous formations. His interpretation was based on detailed logging of the "porphyries", the sedimentary rocks and their contact zones in 23 trenches concentrated along two sections. Teisseyre considered that the lower part of the main (middle) porphyry sheet is a 4 m thick rhyolite lava with abundant pebbles – xenoliths derived from the underlying sediments – as well as molds of *Calamites* twigs. Above, a 1.5 m thick layer of "pisolitic tuff" overlain by another rhyolitic lava, up to 25 m thick, were identified. This "older volcanic assemblage" is overlain by some 15–20 m of conglomerates and mudstones, followed by the "younger volcanic assemblage". The latter, up to 18 m thick, comprises a trachybasalt lava with a rough, uneven top, overlain by a dellenite lava. Overall, Teisseyre (1966) considered that the rocks described represent the oldest volcanic products in the Intra-Sudetic Basin; this early volcanism comprised at least two main episodes of lava effusion, with an explosive eruption and deposition of fall-out tuff with accretionary lapilli during the older episode.

Further support for the above interpretation was provided by petrographic studies of the Sady Górne Culm deposits. Teisseyre (1970) found that all these rocks, especially the finer-grained lithologies, contain a significant volcanogenic component, locally exceeding 50% by volume. The author linked this component with contemporaneous, dominantly silicic volcanism. Westward transport directions in the Sady Górne Culm, together with a westwards decrease of the volcanogenic component in the deposits, suggested that a contemporaneous volcano was located east of the basin.

Awdankiewicz (1999*a*, *b*) distinguished the volcanic rocks of the Sady Górne area as the SGRd and, following Teisseyre (1970), suggested that they were erupted from a volcano located east of the village of Sady Górne where several dykes of

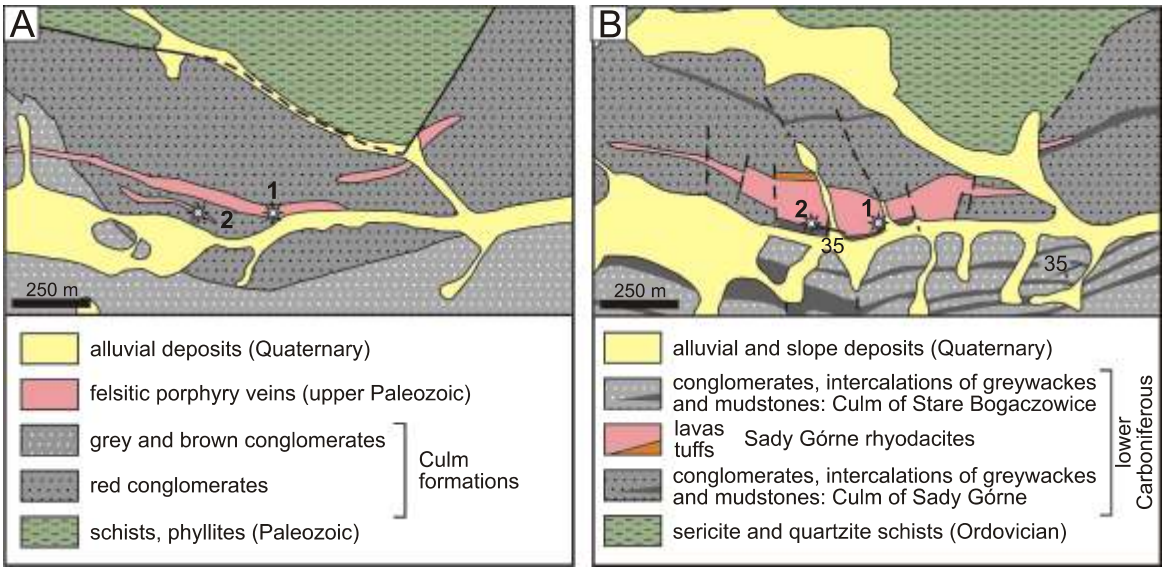

Fig. 2. Geological maps of the study area

A – modified from Berg *et al*. (1906); **B** – based on Teisseyre (1972) and Teisseyre (1966); classification of the volcanic rocks after Awdankiewicz (1999*a*, *b*); star symbols annotated 1 and 2 – localities described in this paper; geographic coordinates of the localities: 1 – N 50°51.549', E 16°10.624'; 2 – N 50°51.554', E 16°10.413'

"porphyries" straddle the fault-bounded margin of the Intra-Sudetic Basin and may represent feeders of an eroded silicic volcano. A geochemical and petrographic study showed that the SGRd are characterized by variable phenocryst contents, groundmass textures and degrees of post-magmatic alteration, and can be subdivided into two main lithologies: phenocryst-poor and phenocryst-rich rhyodacites. The SGRd, together with the Trójgarb rhyolites, Chełmiec and Stary Lesieniec rhyodacites, Nagórnik andesites and Borówno basaltic andesites form the older (Carboniferous) calc-alkaline volcanic suite of the Intra-Sudetic Basin (Awdankiewicz, 1999*a*, *b*).

RESULTS

FIELD RELATIONSHIPS, STRUCTURES AND PETROGRAPHY

The Sady Górne Formation in the study area is *ca*. 400 m thick and dips at *ca*. 35° to the south/south-west, and it consists mainly of medium-grained conglomerates with intercalations of fine-grained conglomerate, siltstone and subgraywacke (Teisseyre, 1966). The lowermost of the three rhyodacite sheets mapped by Berg *et al*. (1906), in the NE part of the study area, is not exposed and was not included in this study. The middle, main rhyodacite sheet extends from west to east for *ca*. 1.5 km, largely subparallel to the stratification of the host deposits, and is up to 20–30 m thick. Some 15 m up-sequence, the uppermost rhyodacite sheet is found. It is up to *ca*. 18 m thick and can be traced for *ca*. 300 m. The main rhyodacite sheet is built up of phenocryst-poor rhyodacites, whereas the uppermost one comprises phenocryst-rich and phenocryst-poor rhyodacites. Detailed petrography and bulk-rock analyses are given by Awdankiewicz (1999*a*, *b*).

Apart from scarce and very small rock crags, the rhyodacites are exposed in two small abandoned quarries (localities 1 and 2, Fig. 2). Locality 1 is situated in the eastern part of the middle rhyodacite sheet, which is probably not more than *ca*. 12–13 m thick there. However, the margins and the contacts with the host deposits are not exposed. The section, *ca*. 10 m thick (Fig. 3, Log 1), shows phenocryst-poor rhyodacites with well-developed columnar joints and less distinctive platy joints perpendicular to the columnar joints. The columns, typically a few cm in diameter, dip to the NNE at *ca*. 40–60°, presumably perpendicular to the margins of the rhyodacite sheet. The platy joints dip to the SSW at 25–30°, probably subparallel to the margins of the sheet. Flow lamination, subparallel to the platy joints, is common. Indistinct cm-sized flow folds occur in places. Columnar joints become less regular in the lower part of this section. The uppermost 3 m of the section is more heterogeneous and consists of aligned domains, decimetres thick and metres long, of alternating columnar-jointed rhyodacites and platy-jointed rhyodacites. The columnar-jointed domains are structurally equivalent to the underlying part of the section. The platy-jointed domains are characterized by wide, wavy undulations as well as indistinct, aligned zones of dense fracturing and brecciation, with angular rhyodacite clasts less than 1 cm in size.

Locality 2 is situated in the eastern part of the uppermost rhyodacite sheet (Fig. 2). The sheet is between 10 and 20 m thick there, and a *ca*. 4 m thick section of the inner part of the sheet can be observed (Fig. 3, Log 2). The lower part of the section consists of a phenocryst-rich rhyodacite and the upper part is built of phenocryst-poor rhyodacite. The contact of these two lithologies is sharp and uneven, with a vertical relief of up to *ca*. 2–3 m in amplitude. Teisseyre (1966) noted differences in joint patterns in the two lithologies. Indeed, the phenocryst-rich

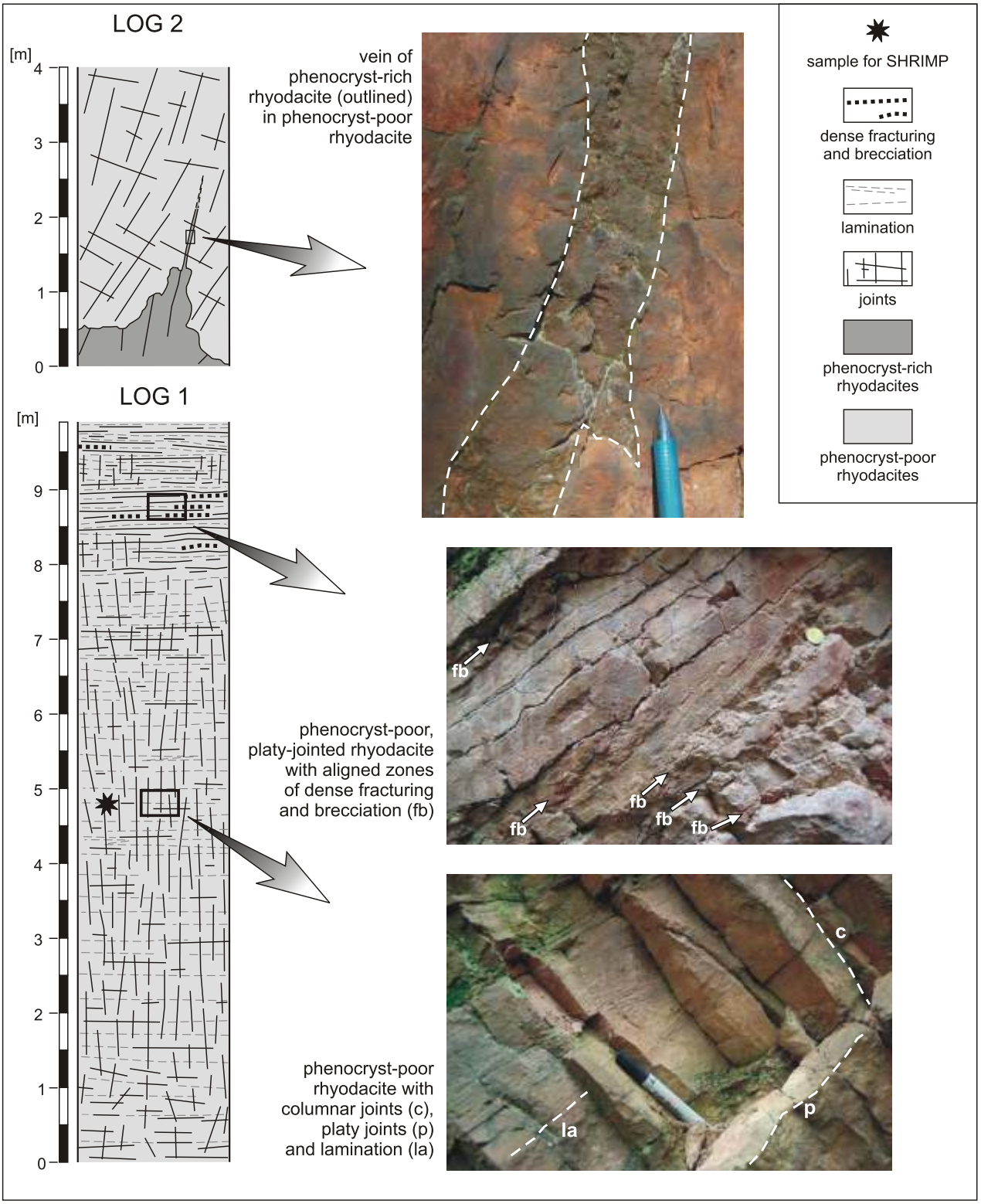

Fig 3. Logs and photos illustrating structures and textures of rhyodacites at localities 1 and 2

Comments in text

rhyodacite shows blocky-type joints, with most joint planes trending perpendicular to the contact with the overlying phenocryst-poor rhyodacite. The latter is characterized by more densely spaced and less regular joints. In addition, detailed re-examination of the southeastern part of the quarry reveals a 4–5 cm thick vein of the phenocryst-rich rhyodacite penetrating into the phenocryst-poor rhyodacite from the top of a wider "ridge" of the phenocryst-rich rhyodacite (Fig. 3, Log 2). A similar but thicker apparent vein, with more diffuse and wavy margins and seen in a section subparallel to its strike,

occurs in the central part of the quarry. Neither well-defined chilled margins nor enclaves of one rhyodacite type in the other were found.

The phenocryst-poor rhyodacites are pale pink to reddish, aphanitic, nearly aphyric rocks with light and dark laminae, 1–20 mm thick. Sparse and small phenocrysts (*ca*. 1% by volume and less than 0.7 mm in size) comprise quartz, altered feldspars and biotite. Primary feldspars are usually replaced by albite and kaolinite, whereas the biotite is partly chloritized and intergrown by sericite aggregates. The microcrystalline groundmass consists of quartz, alkali feldspars, biotite, sericite, kaolinite and opaques. Lamination is due to variable amounts of aligned kaolinite and quartz streaks and variable amounts of Fe-rich "pigment". Most specimens also show alignment of phenocrysts and of groundmass biotite plates. At locality 1, an indistinct microspherulitic texture is locally developed. The microspherulites, *ca*. 0.05–0.1 mm in diameter, are composed of quartz and alkali feldspars, with the cores more intensely stained by Fe-rich pigment and the margins outlined by concentrations of sericite or quartz and kaolinite aggregates.

The fractured and brecciated domains at locality 1 show various textures. In places there are relatively well-defined subangular to subrounded rhyodacite fragments, up to few milimetres in size. The clasts differ from the host rock in their groundmass texture (e.g., felsitic-textured clasts in microspherulitic rhyodacites). Some clasts show internal lamination which is rotated relative to the lamination in the host rhyodacite. There are also networks of anastomosing, cross-cutting, sericite-enriched veinlets and patches, which result in microbrecciated, jigsaw-textured domains. Locally, there are opaque patches rich in Fe-oxide pigment.

The phenocryst-rich rhyodacites contain *ca*. 15% (vol.) of phenocrysts which are up to 3 mm long and are set in a microcrystalline, massive to trachytic-textured groundmass. Apart from biotite, which shows thin, discontinuous, opaque-rich reaction rims, the other phenocrysts are pseudomorphs after plagioclase and mafic minerals. Plagioclase is replaced by albite and kaolinite and shows relics of polysynthetic twins, sieve textures (groundmass inclusions) and zoning (variable distribution of the post-magmatic minerals). The mafic pseudomorphs consist mainly of kaolinite and opaques. The prismatic, six-sided habit and thick, opaque outlines of many pseudomorphs suggest that the original igneous mineral was hornblende, which was partly decomposed into "opacite" along the margins. A porous appearance of the rhyodacites in hand-specimen results from leaching of the pseudomorphs on weathering. The groundmass of the phenocryst-rich rhyodacites is mainly composed of aligned laths, *ca*. 0.05 mm long, of albitized and sericitized plagioclase. The other components include anhedral alkali feldspars and quartz, kaolinite and sericite flakes, opaque grains and acicular crystals of apatite.

ZIRCON STUDY AND SHRIMP AGES

A number of zircon grains are short prismatic, subhedral to subrounded (Fig. 4) and a few of these yielded inherited ages (grains 6.1, 7.1, 11.1, 13.1; see below). The majority of grains

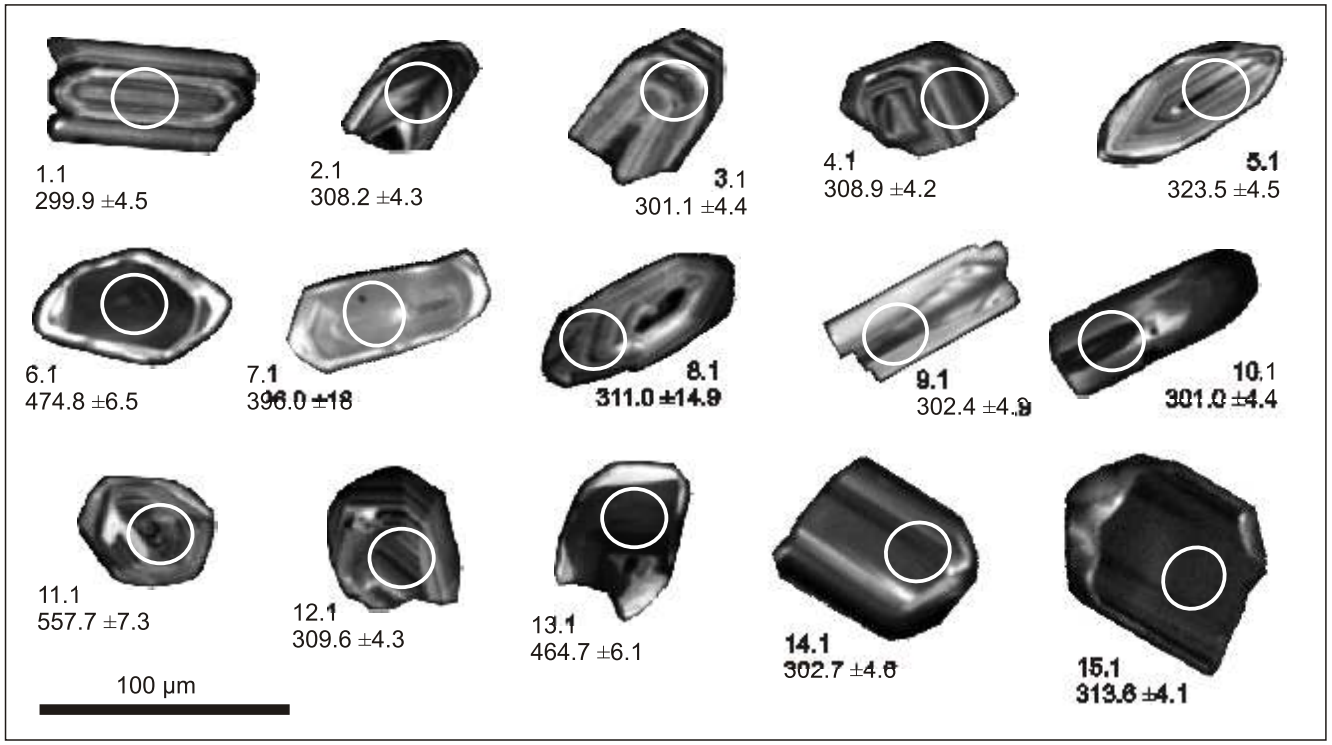

Fig. 4. Cathodoluminescence images of zircons from the rhyodacite

Elliptical analytical spots are *ca*. 30 micrometers large;
$^{206}Pb/^{238}U$ ages given in labels are common Pb corrected using measured ^{204}Pb and 1σ errors

form a fairly homogeneous population of short- to normal-prismatic crystals, euhedral to subhedral, partly broken. Typically, they show distinct "magmatic" zoning, consistent with their volcanic derivation. However, particular grains display various features testifying to their complex origin. Grains 6.1, 7.1 and 13.1 are subrounded, with CL bright rims and indistinct cores representing inherited components. Relatively larger grains 14.1 and 15.1, with banded zonation possibly reflecting crystallisation from more mafic magma, might represent a pre-eruptive history (but we should keep in mind that this observation is based only on a few, rather exceptional grains in the zircon separate investigated). The most abundant prismatic crystals, with fine-scale oscillatory zonation (1.1, 2.1, 3.1, 4.1, 5.1, 8.1, 9.1, 10.1, 12.1), most likely represent the main population that crystallised from felsic magma.

Based on transmitted and reflected light, and cathodoluminescence (CL) images, fifteen points in fifteen grains have been selected for SHRIMP analysis (Fig. 4 and Table 1). One point (7.1), CL-bright, U- and Th-poor, and with high common lead (3.73% $^{206}Pb_c$), is strongly discordant (discordance D = 100 [(age $^{207}Pb/^{206}Pb$)/(age $^{206}Pb/^{238}U$) – 1] = – 50%) and has been excluded from our interpretation.

Three grains yielded ages distinctly older than the main zircon population. The oldest grain (11.1, Table 1) shows a $^{206}Pb/^{238}U$ age of 558 ±7 Ma but it is slightly discordant (D = 10), thus its true age may be somewhat older ($^{207}Pb/^{206}Pb$ age is 614 ±34 Ma). The grain is a subrounded, transparent crystal, with recurrent "magmatic" zoning. Its $^{232}Th/^{238}U$ ratio is 0.28.

The two other inherited grains, 6.1 and 13.1, yielded similar, within error, $^{206}Pb/^{238}U$ ages of 475 ±6 and 465 ±6 Ma, respectively (Fig. 5A). They are also slightly positively discordant ($^{207}Pb/^{206}Pb$ ages of 521 ±37 and 520 ±37 Ma, respectively). The average concordia age of these two points is 471 ±9 Ma. Both the grains are subrounded and display similar internal structure: CL-dark homogeneous interiors and thin CL-bright rims (Fig. 4). Both the grains have high $^{232}Th/^{238}U$ ratios (0.52 and 0.43), typical of magmatic zircons.

Grain 5.1 with a $^{206}Pb/^{238}U$ age of 323 ±4 Ma is considerably older than the main zircon population. Its rather high positive discordance (D = 35) suggests that the $^{207}Pb/^{206}Ub$ age of 435 ±70 Ma approximates the minimum age of that crystal.

The main population of zircons comprises ten analytical points with $^{206}Pb/^{238}U$ ages within the range of 300 ±4 Ma (grain 1.1) and 314 ±4 Ma (grain 15.1), all concordant within 2 σ errors (Fig. 5B). The average concordia age for this group is 306.1 ±2.8 Ma. Most of these grains have similar morphology, they are euhedral or subhedral short- to normal-prismatic transparent crystals, usually with distinct recurrent CL zoning. They also display moderate to fairly high $^{232}Th/^{238}U$ ratios, between 0.22 and 0.96.

Table 1

SHRIMP zircon data from rhyodacite SG from Stare Bogaczowice

Spot	$^{206}Pb_c$ [%]	U [ppm]	Th [ppm]	$^{232}Th/^{238}U$	$^{206}Pb^*$ [ppm]	(1) $^{206}Pb/^{238}U$ Age		$^{207}Pb/^{206}Pb$ Age		Discordant [%]	Total $^{238}U/^{206}Pb$	± [%]	Total $^{207}Pb/^{206}Pb$	± [%]	(1) $^{207}Pb^*/^{206}Pb^*$	± [%]	(1) $^{207}Pb^*/^{235}U$	± [%]	(1) $^{206}Pb^*/^{238}U$	± [%]	err. corr.
1.1	0.45	409	158	0.40	16.8	299.9	±4.5	312	±140	4	20.9	1.5	0.0562	2.1	0.0526	6.0	0.345	6.2	0.04762	1.5	.249
2.1	0.00	400	185	0.48	16.8	308.2	±4.3	304	±53	–1	20.43	1.4	0.0519	2.2	0.0524	2.3	0.354	2.7	0.04897	1.4	.521
3.1	0.00	360	128	0.37	14.8	301.1	±4.4	388	±65	29	20.95	1.5	0.0531	2.2	0.0544	2.9	0.359	3.3	0.04781	1.5	.462
4.1	0.26	547	115	0.22	23.1	308.9	±4.2	341	±66	11	20.32	1.4	0.05541	1.7	0.0533	2.9	0.361	3.2	0.04908	1.4	.428
5.1	0.00	476	360	0.78	21.0	323.5	±4.5	435	±70	35	19.48	1.4	0.0538	2	0.0556	3.1	0.394	3.5	0.05146	1.4	.410
6.1	0.00	369	186	0.52	24.2	474.8	±6.5	521	±37	10	13.08	1.4	0.05778	1.7	0.05778	1.7	0.609	2.2	0.0764	1.4	.648
7.1	3.73	18	6	0.35	1.04	396.0	±18	200	±1300	–50	15.19	2.9	0.0798	9.7	0.05	58.1	0.44	58.1	0.0634	4.6	.079
8.1	0.56	232	58	0.26	9.89	311.0	±4.9	260	±120	–16	20.12	1.6	0.0559	2.6	0.0514	5.3	0.35	5.5	0.04943	1.6	.293
9.1	0.33	145	90	0.65	5.98	302.4	±4.9	216	±120	–29	20.75	1.6	0.0531	3.4	0.0505	5.1	0.334	5.4	0.04803	1.7	.306
10.1	0.00	387	358	0.96	15.8	301.0	±4.4	443	±68	47	20.98	1.5	0.0535	2.2	0.0558	3.1	0.367	3.4	0.04781	1.5	.438
11.1	0.00	499	134	0.28	38.7	557.7	±7.3	614	±34	10	11.08	1.4	0.05936	1.3	0.06029	1.6	0.751	2.1	0.0904	1.4	.657
12.1	0.00	510	125	0.25	21.6	309.6	±4.3	298	±43	–4	20.32	1.4	0.0523	1.9	0.0523	1.9	0.3548	2.4	0.04921	1.4	.604
13.1	0.00	517	215	0.43	33.1	464.7	±6.1	520	±37	12	13.39	1.4	0.05713	1.4	0.05776	1.7	0.595	2.2	0.0747	1.4	.626
14.1	0.48	332	236	0.73	13.8	302.7	±4.6	403	±120	33	20.7	1.5	0.0586	2.2	0.0548	5.6	0.363	5.8	0.04807	1.5	.267
15.1	0.24	1319	483	0.38	56.6	313.6	±4.1	303	±63	–3	20.01	1.3	0.05432	1.2	0.0524	2.7	0.36	3.0	0.04985	1.3	.436

Errors are 1 σ; Pb_c and Pb^* – indicate the common and radiogenic portions, respectively; error in standard calibration was 0.44%; (1) – common Pb corrected using measured ^{204}Pb

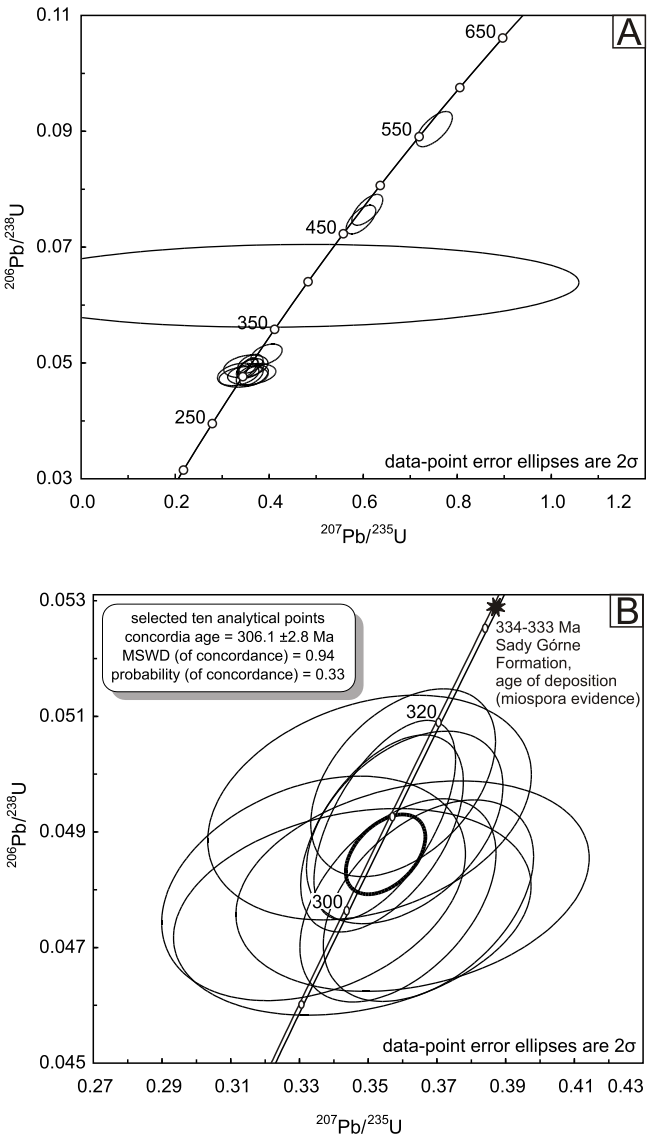

Fig. 5A – concordia diagram for rhyodacite sample SG, all 15 measured points; B – concordia diagram for ten selected analytical points of the main age population of zircons

The age of deposition of the host sedimentary rocks of the rhyodacites, the Sady Górne Formation, after Turnau *et al*. (2002)

DISCUSSION

GEOLOGICAL FORM AND EMPLACEMENT PROCESSES OF THE RHYODACITES

Two contrasting interpretations of the geological form and emplacement processes of the Sady Górne rhyodacites have been proposed so far: Berg *et al*. (1906) considered that these are intrusive veins, whereas Teisseyre (1966) argued that these are lavas and tuffs. Criteria for distinction between subvolcanic intrusions and extrusions in modern and ancient sequences have been discussed in detail by McPhie *et al*. (1993); the criteria relay on the geometry and internal structures of the igneous bodies and, in particular, on the lithologies and textures in marginal and contact zones of such igneous bodies. However, a sharp division into lavas *sensu stricto* and subvolcanic intrusions is not always possible even in modern successions, where transitional types of (sub)volcanic bodies such as cryptodomes are found (e.g., Cas and Wright, 1987). In ancient sequences, such factors as tectonics, erosion, alteration or metamorphism may further obscure original emplacement-related characteristics.

The interpretation of the SGRd is mainly hampered by limited exposure, and the information on margins and contact zones of the rhyodacites comes only from Teisseyre's (1966) descriptions from trenches. However, the data available are more consistent with the emplacement of the rhyodacites as intrusive sheets.

The Sady Górne rhyodacites sheets seem largely conformable, but the westernmost part of the longest sheet may be unconformable (Fig. 2A). Similarly, the platy joints at locality 1, presumably subparallel to the margins of this sheet, dip at a higher angle than the host sedimentary rocks. Therefore it is possible that the rhyodacite sheet is slightly discordant and cuts bedding in the host rocks at a low angle. Such relationships could not be found if the rhyodacites were lavas.

The thickness of individual rhyodacite sheets varies from a few to *ca*. 30 m. Even the highest of these values are relatively low for silica-rich (dacitic-rhyolitic) lava flows, and it is unlikely that such only meters-thick sheets were emplaced as lavas (*cf*. Cas and Wright, 1987; McPhie *et al*., 1993).

Observations from the exposures and from trenches (Teisseyre, 1966) show that the SGRd are almost exclusively represented by aphanitic to porphyrytic, microcrystalline rocks. Such lithologies are typical of intrusive sheets. Various types of joints, lamination and minor zones of breccias can be linked with flowage and cooling of magma, and localized cracking of solidifying rhyodacite, in the intrusive sheets. In contrast, silicic lava flows are characterized by much stronger lithological and petrographic variation in vertical sections (Cas and Wright, 1987; McPhie *et al*., 1993; Paulick and Breitkreuz, 2005 and references therein). The marginal "carapace facies" lithologies (autoclastic breccias, obsidian, spherulitic rhyolites) are abundant or even predominate over the inner "core facies" (microcrystalline rhyolites). In this context the "pisolitic tuffs" and "lava-cemented conglomerates" described by Teisseyre (1966) from the lower part of his "older volcanic assemblage" may also be interpreted as some marginal facies lithologies developed along the thickest part of the intrusive sheet. The origin of the "lava-cemented conglomerates" due to the interaction of rhyodacite magma with unconsolidated pebbly deposits in the contact zone (Teisseyre, 1966) seems essentially correct. However, it is equivocal or doubtful whether the "lapilli tuff" does really represent a pyroclastic rock, or rather some other fragmental to coherent rock, such as altered, (?)partly autobrecciated, spherulitic, hypocrystalline rhyodacite. In fact Teisseyre (1966) reports that no ash particles could be observed in thin sections of the "tuffs".

Arguments similar to those above may be also raised against the interpretation of the upper rhyodacite sheet as two successive lava flows. Furthermore, the vein(s) of phenocryst-rich rhyodacite cutting the phenocryst-poor

rhyodacite (Fig. 3, Log 2) show that the relative age of these lithologies is opposite to that expected for two successive lava flows. It is therefore suggested that this rhyodacite sheet represents a composite vein formed by successive emplacement of two main magma batches: the phenocryst-poor magma first and the phenocryst-rich magma next. The second magma batch disrupted and intruded the earlier, partly solidified magma, and could have been cooled against the earlier, already solidified domains, which resulted in the observed rough contacts, veins and joint patterns.

Another problem is the origin of the volcanogenic material in deposits of the Sady Górne Formation (Teisseyre, 1970). This is beyond the scope of this study, but it should be noted that the similarity between this "tuffaceous" volcanogenic component and the SGRd is not definitely confirmed, e.g. by trace element chemistry or by mineral chemistry data. Therefore, the relationship to any possible contemporaneous volcano in this region, or to other more remote and unrelated sources, is not well-constrained.

Overall, the re-examination of field relationships presented in this study provides arguments for the subvolcanic emplacement of the SGRd, as a set of intrusive, conformable to semiconformable(?) sheets, some of composite nature. This is generally consistent with the original interpretation of Berg *et al*. (1906).

AGE OF RHYODACITES

Our SHRIMP analyses did not aim at detailed deciphering of the entire spectrum of inherited zircons in the Stare Bogaczowice rhyodacites, however, a few analyses obtained from subrounded zircon grains (6.1, 13.1 and 11.1) confirm the presence of inherited materials in these rocks. They seem to represent two crustal sources of various ages: (a) of *ca*. 560 Ma, and (b) of *ca*. 470 (or slightly older) Ma. These broadly correspond to, respectively, the Cadomian and lower Ordovician granitoids/orthogneisses exposed in a number of basement units of the Sudetes (we should notice, however, that the lower Ordovician orthogneisses exposed in the neighbourhood are significantly older, i.e. *ca*. 490–500 Ma; Pin *et al*. (2007) and inferred to form parts of the underlying middle crust of this region (Oberc-Dziedzic *et al*., 2009). The rhyodacites may contain materials derived by partial melting of such crustal sources or they have been significantly contaminated by that sort of felsic rocks. An alternative, more complex scenario could be that the older zircons were first supplied into the sediments of the Intra-Sudetic Basin as detritus derived from basement outcrops, and then incorporated by the ascending SGRd magma from the sedimentary country rocks.

The main population of the zircons in the rhyodacites is homogenous in morphology, internal structures and a range of chemical/isotopic characteristics. In particular, their euhedral and prismatic habit, recurrent zonation, together with the relatively high $^{232}Th/^{238}U$ ratios (between 0.22 and 0.96), indicate their magmatic crystallisation. The average concordia age of 306.1 ±2.8 Ma is interpreted as corresponding to the main magmatic crystallisation of the rhyodacitic magma. The magmatic age of the rhyodacites, based on our SHRIMP data, corresponds to the Westphalian (Menning *et al*., 2006).

REGIONAL IMPLICATIONS

The results presented in this paper, together with the biostratigraphic dating of the early Carboniferous deposits of the Intra-Sudetic Basin (Turnau *et al*., 2002), show that the Sady Górne rhyodacites were emplaced in the late Carboniferous, *ca*. 24–31 My after the deposition of their host rocks. This cast doubts on the current views on the early phases of volcanism in the Intra-Sudetic Basin (Teisseyre, 1966; Awdankiewicz, 1999*a*, *b*). Possibly, volcanism in the Intra-Sudetic Basin was initiated several million years later than supposed so far. The Sady Górne rhyodacite can no longer be linked with some initial, early Carboniferous volcanic phase, but apparently with a younger, late Carboniferous phase of volcanism. A preliminary SHRIMP zircon dating of the rhyodacitic Chełmiec laccolith near Wałbrzych suggests its emplacement at *ca*. 310 Ma (Awdankiewicz and Kryza, 2010). An older SHRIMP zircon age of *ca*. 315 Ma has been obtained for rhyodacites of the Żeláźniak subvolcanic intrusion cutting the basement rocks of the Intra-Sudetic Basin to the north-west (Machowiak *et al*., 2008). The relatively large spread in the ages obtained so far suggests a relatively prolonged phase and several pulses of late Carboniferous magmatism in the Intra-Sudetic Basin and its vicinity, but the questions of when the volcanism was initiated and how long it lasted cannot yet be answered precisely as some other (sub)volcanic rock units to the west and south-west of the SGRd (e.g., the Trójgarb rhyolites and the Nagórnik andesites) remain undated.

CONCLUSION

The key results of this study can be summarized as follows:

1. The Sady Górne rhyodacites were emplaced as intrusive, conformable to semiconformable, simple to composite sheets into the conglomerates and mudstones of the Sady Górne Formation, in the lowermost part of the molasse fill of the Intra-Sudetic Basin.

2. A SHRIMP zircon study of the rhyodacites reveals a few inherited zircons of *ca*. 560 Ma, and *ca*. 470 Ma, derived from contaminants or source rocks of the rhyodacite magma. The main population of zircons, dated at 306.1 ±2.8 Ma, reflects the emplacement age of the rhyodacites in the mid to late part of the late Carboniferous (Westphalian), some 24–31 My after the deposition of their host rocks.

3. The new results cast doubts on the current views on the timing of late- and post-orogenic volcanism in the Intra-Sudetic Basin in the Central European Variscides. Possibly, this volcanism was initiated in the late, not in the early Carboniferous, several million years later than assumed so far.

Acknowledgements. A zircon separate from a sample of the Sady Górne rhyodacites obtained by M. Jurasik for her MSc project was used for our SHRIMP study, performed in VSEGEI, St. Petersburg. Prof. A. Majerowicz helped to translate German publications. The study was financially supported by Wrocław University internal grants, 2022/W/ING and 1017/S/ING, and from MNiSW grant N N307 055037. The paper has been constructively reviewed by Ch. Breitkreuz and E. Krzemińska. All these individuals and institutions are greatly acknowledged for their help and support.

REFERENCES

AWDANKIEWICZ M. (1999*a*) – Volcanism in a late Variscan intramontane trough: Carboniferous and Permian volcanic centres of the Intra-Sudetic Basin, SW Poland. Geol. Sudet., **32** (1): 13–47.

AWDANKIEWICZ M. (1999*b*) – Volcanism in a late Variscan intramontane trough: the petrology and geochemistry of the Carboniferous and Permian volcanic rocks of the Intra-Sudetic Basin, SW Poland. Geol. Sudet., **32** (2): 83–111.

AWDANKIEWICZ M. (2004) – Sedimentation, volcanism and subvolcanic intrusions in a late Palaeozoic intramontane trough (the Intra-Sudetic Basin, SW Poland). Geol. Soc., London, Spec. Publ., **234**: 5–11.

AWDANKIEWICZ M. and KRYZA R. (2010) – The Chełmiec subvolcanic intrusion (Intra-Sudetic Basin, SW Poland): preliminary SHRIMP zircon age. Miner. Spec. Pap., **37**.

BERG G., DATHE E. and ZIMMERMANN E. (1906) – Geologischen Karte von Preußen und benachbarten Bundesstaaten. Blatt Freiburg., Berlin.

BLACK L. P., KAMO S. L., ALLEN C. M., ALEINIKOFF J. N., DAVIS D. W., KORSCH R. J. and FOUDOULIS C. (2003) – TEMORA 1: a new zircon standard for Phanerozoic U-Pb geochronology. Chem. Geol., **200**: 155–170.

BOSSOWSKI A., SAWICKI L. and WROŃSKI J. (1981) – Mapa geologiczna Polski 1:200 000. B – mapa bez utworów czwartorzędowych, ark. Wałbrzych. Wyd. Geol., Warszawa.

CAS R. A. F. and WRIGHT J. V. (1987) – Volcanic successions modern and ancient: a geological approach to processes, products and successions. Allen and Unwin Ltd.

DATHE E. and ZIMMERMANN E. (1912) – Erläuterungen zur geologischen karte von Preußen und benachbarten Bundesstaaten. Blatt Freiburg (Lieferung 145). Königliche Geologische Landesanstalt, Berlin.

DZIEDZIC K. and TEISSEYRE A. K. (1990) – The Hercynian molasse and younger deposits in the Intra-Sudetic Depression, SW Poland. Neues Jahrb. Geol. Paläont. Abh., **179**: 285–305.

JURASIK M. (2006) – Zircons from the Lower Carboniferous volcanic rocks of the Intra-Sudetic Basin and bentonites of the Bardo Mountains (in Polish with English summary). Unpubl. M.Sc. thesis, University of Wrocław.

KODYM O., FUSÁN O. and MATĚJKA A., eds. (1967) – Geological Map of Czechoslovakia 1:500 000, West. Ústředni ústav geologický, Praha.

LARIONOV A. N., ANDREICHEV V. A. and GEE D. G. (2004) – The Vendian alkaline igneous suite of northern Timan: ion microprobe U-Pb zircon ages of gabbros and syenite. Geol. Soc. London Mem., **30**: 69–74.

LUDWIG K. R. (2005*a*) – SQUID 1.12 A User's Manual. A Geochronological Toolkit for Microsoft Excel. Berkeley Geochronol. Center Spec. Publ.: 1–22, http://www.bgc.org/klprogrammenu.html

LUDWIG K. R. (2005*b*) – User's Manual for ISOPLOT/Ex 3.22. A Geochronological Toolkit for Microsoft Excel. Berkeley Geochronol. Center Spec. Publ.: 1–71, http://www.bgc.org/klprogrammenu.html.

MACHOWIAK K., ARMSTRONG R., KRYZA R. and MUSZYŃSKI A. (2008) – Late-orogenic magmatism in the central European Variscides: SHRIMP U-Pb zircon age constraints from the Żelaźniak intrusion, Kaczawa Mountains, West Sudetes. Geol. Sudet., **40**: 1–18.

MASTALERZ K. and PROUZA V. (1995) – Development of the Intra-Sudetic Basin during Carboniferous and Permian. In: Sedimentary Record of the Variscan Orogeny and Climate – Intra-Sudetic Basin, Poland and Czech Republic (eds. K. Mastalerz, V. Prouza, L. Kurowski, A. Bossowski, A. Ihnatowicz and G. Nowak): 5–15. Guide to Excursion B1. XIII International Congress on Carboniferous-Permian. August 28–September 2, 1995, Karków, Poland.

McPHIE J., DOYLE M. and ALLEN R. (1993) – Volcanic textures. A guide to the interpretation of textures in volcanic rocks. CODES, Tasmania.

MENNING M., ALEKSEEV A. S., CHUVASHOV B. I., DAVYDOV V. I., DEVUYST F. X., FORKE H. C., GRUNT T. A., HANCE L., HECKEL P. H., IZOKH N. G., JIN Y. G., JONES P. J., KOTLYAR G. V., KOZUR H. W., NEMYROVSKA T. I., SCHNEIDER J. W., WANG X. D., WEDDIGE K., WEYER D. and WORK D. M. (2006) – Global time scale and regional stratigraphic reference scales of Central and West Europe, East Europe, Tethys, South China, and North America as used in the Devonian-Carboniferous-Permian Correlation Chart 2003 (DCP 2003). Palaeogeogr. Palaeoclimat. Palaeoecol., **240**: 318–372.

MILEWICZ J., SZAŁAMACHA J. and SZAŁAMACHA M. (1989) – Mapa geologiczna Polski 1:200 000. B – mapa bez utworów czwartorzędowych, ark. Jelenia Góra. Wyd. Geol., Warszawa.

NEMEC W., PORĘBSKI S. and TEISSEYRE A. K. (1982) – Explanatory notes to the lithotectonic molasse profile of the Intra-Sudetic Basin, Polish Part (Sudety Mts., Carboniferous-Permian). Veröffentlichung des Zentralinstituts für Physik der Erde AdW DDR, Potsdam, **66**: 267–277.

OBERC-DZIEZIC T., KRYZA R. and PIN C. (2009) – The crust beneath the Polish Sudetes: evidence from a gneiss xenolith in Tertiary basanite from Paszowice. Geodinam. Acta, **22** (3): 9–31.

PAULICK H. and BREITKREUZ C. (2005) – The Late Palaeozoic felsic lava-dominated large igneous province in northeast Germany: volcanic facies analysis based on drill cores. Internat. J. Earth Sc., **94**: 834–850.

PIN C., KRYZA R., OBERC-DZIEDZIC T., MAZUR S., TURNIAK K. and WALDHAUSROVÁ J. (2007) – The diversity and geodynamic significance of Late Cambrian (c. 500 Ma) felsic anorogenic magmatism in the northern part of the Bohemian Massif: a review based on Sm–Nd isotope and geochemical data. Geol. Soc. Am. Spec. Publ., **423**: 209–230.

SAWICKI L. (1988) – Mapa geologiczna Polski 1:200 000. B – mapa bez utworów czwartorzędowych, ark. Kłodzko. Wyd. Geol., Warszawa.

STACEY J. S. and KRAMERS J. D. (1975) – Approximation of terrestrial lead isotope evolution by a two-stage model. Earth Planet. Sc. Lett., **26**: 207–221.

STEIGER R. H. and JÄGER E. (1977) – Subcommission on geochronology: convention on the use of decay constants in geo- and cosmochronology. Earth Planet. Sc. Lett., **36**: 359–362.

TEISSEYRE A. K. (1966) – On the Lower Carboniferous volcanism of the Intrasudetic Basin: new data about eruptive and pyroclastic rocks (in Polish with English summary). Acta Geol. Pol., **16** (4): 445–475.

TEISSEYRE A. K. (1968) – The Lower Carboniferous of the Intrasudetic Basin: a study in sedimentary petrology and basin analysis (in Polish with English summary). Geol. Sudet., **4**: 221–298.

TEISSEYRE A. K. (1970) – Contemporaneous pyrogenic materials in the Kulm of Sady Górne (Intrasudetic Basin). Bull. Pol. Sc., Sér. Sc. Géol. Géogr., **18** (1): 21–27.

TEISSEYRE A. K. (1975) – Sedimentology and palaeogeography of the Kulm alluvial fans in the western Intrasudetic Basin (Central Sudetes, SW Poland) (in Polish with English summary). Geol. Sud., **9**.

TEISSEYRE H. (1972) – Szczegółowa mapa geologiczna Sudetów 1:25 000, ark. Stare Bogaczowice. Wyd. Geol., Warszawa.

TURNAU E., ŻELAŹNIEWICZ A. and FRANKE W. (2002) – Middle to early late Visean onset of late orogenic sedimentation in the Intra-Sudetic Basin, West Sudetes: miospore evidence and tectonic implications. Geol. Sudet., **34**: 9–16.

ULRYCH J., FEDIUK F., LANG M. and MARTINEC P. (2004) – Late Palaeozoic volcanic rocks of the Intra-Sudetic Basin, Bohemian Massif: petrological and geochemical characteristics. Chemie der Erde, Geochem., **64**: 127–153.

WAGNER R., ed. (2008) – Tabela stratygraficzna Polski. Polska pozakarpacka. Ministerstwo Środowiska, Warszawa.

WIEDENBECK M., ALLÉ P., CORFU F., GRIFFIN W. L., MEIER M., OBERLI F., von QUADT A., RODDICK J. C. and SPIEGEL W. (1995) – Three natural zircon standards for U-Th-Pb, Lu-Hf, trace element and REE analyses. Geostandard Newslett., **19**: 1–23.

WILLIAMS I.S. (1998) – U-Th-Pb Geochronology by ion microprobe. Soc. Econom. Geol., Rev. Econom. Geol., **7**: 1–35.

WOJEWODA J. and MASTALERZ K. (1989) – Climate evolution, allo- and autocyclicity of sedimentation: an example from the Permo-Carboniferous continental deposites of the Sudetes, SW Poland (in Polish with English summary). Prz. Geol., **37** (4): 173–180.

ZIMMERMANN E. (1920) – Die Gänge und Stöcke von Porphyr im Katzbach- und Waldenburger Gebirge in Schlesien. Jahrb. Preußisch. Geol. Landesanst., Band XLI, Teil II, Heft, **1**: 356–367.

APPENDIX

SHRIMP analytical procedure

U-Pb analyses were performed on a SHRIMP-II at the Centre of Isotopic Research (CIR) at VSEGEI, applying a secondary electron multiplier in peak-jumping mode following the procedure described in Williams (1998) and Larionov *et al*. (2004). A primary beam of molecular oxygen was employed to ablate zircon in order to sputter secondary ions. The elliptical analytical spots had a size of *ca*. 27 × 20 μm, and the corresponding ion current was *ca*. 4 nA. The sputtered secondary ions were extracted at 10 kV. The 80 μm wide slit of the secondary ion source, in combination with a 100 μm multiplier slit, allowed mass-resolution of M/ΔM >5000 (1% valley) so that all the possible isobaric interferences were resolved. One-minute rastering over a rectangular area of *ca*. 60 × 50 μm was employed before each analysis in order to remove the gold coating and possible surface common Pb contamination.

The following ion species were measured in sequence: $^{196}(Zr_2O)$–^{204}Pb–background (*ca*. 204 AMU) –^{206}Pb–^{207}Pb–^{208}Pb–^{238}U–^{248}ThO–^{254}UO with integration time ranging from 2 to 20 seconds. Four cycles for each spot analysed were acquired. Each fifth measurement was carried out on the zircon Pb/U standard TEMORA (Black *et al*., 2003) with an accepted ^{206}Pb/^{238}U age of 416.75 ±0.24 Ma. The 91500 zircon with a U concentration of 81.2 ppm and a ^{206}Pb/^{238}U age of 1062.4 ±0.4 Ma (Wiedenbeck *et al*., 1995) was applied as a "U-concentration" standard. The collected results were then processed with the *SQUID v1.12* (Ludwig, 2005*a*) and *ISOPLOT/Ex 3.22* (Ludwig, 2005*b*) software, using the decay constants of Steiger and Jäger (1977). The common lead correction was done using measured ^{204}Pb according to the model of Stacey and Kramers (1975).